Semi-Annual Report for January-June, 1998
Kendall L. Carder, University of South Florida
NAS5-31716

Abstract

The algorithm-development activities at USF during the first half of 1998 have concentrated on data collection and theoretical modeling. Six abstracts were presented at the AGU conference in San Diego, California during February 9 –13, 1998. Two abstracts were submitted for presentation: 1) Western Pacific AGU conference in Taipei, Taiwan on July 21-24; 2) PORSEC'98 Qingdao, China on July 26-28, 1998. Seven abstracts were submitted for presentation at the Ocean Optics conference in Hawaii on November 14 – 17, 1998. Four papers were submitted to JGR and Applied Optics for publication.

Tasks Accomplished:

1. Five cruises and one calibration trip were completed.

    a. Florida Bay cruise

        1) January 29 -31, 1998

        2) NOAA funded ship time

        3) Transects inside Florida Bay, SLFMR (Scanning Low Frequency Microwave Radiometer) overflight

        4) Assuming the effects of shallow waters and turbidity on SeaWiFS data.

    b. Lake Okeechobee

        1) February 18, 1998

2) SIMBIOS funded

3) Transects in Lake Okeechobee

3) Determine atmospheric adjacency and stray light effects from surrounding vegetation for NIR bands on SeaWiFS images of Lake Okeechobee , and an evaluation of aerosol radiance at 412 nm using Lake Okeechobee as a dark target.

c. Calibration:

1) March, 1998

2) At U. of Arizona and Mt. Lemmon

3) Calibration of handheld Spectrix spectroradiometers, LICOR downwelling spectal irradiance meter, Microtops II and Reagan solar radiometers, and Spectralon reflectance panel in the lab and using the direct/diffuse solar irrandiance method on Mt. Lemmon (Biggar et al., 1994).

d. Tongue of the Ocean research campaign

1) April 1- 7, 1998

2) NASA-SIMBIOS-funded ship time with some MODIS funded personnel

3) Transects along and offshore from shallow banks of the Tongue of the Ocean in the Bahamas and out to clear water.

4) Assessment of atmospheric adjacency effects and stray light due to bright bank effects on dark targets using SeaWiFS data. Chlorophyll *a* (Chl), particle absorption coefficients (a_p), detritus absorption coefficients (a_d), gelbstuff absorption coefficients (a_g), backscattering coefficients, shadow-band sky radiometry, water-leaving radiance (L_w), downwelling irradiance(E_d), diffuse

attenuation coefficients(K_d) remote sensing reflectance (R_{rs}) were collected at station locations, while chlorophyll fluorescence, attenuation coefficients (c), salinity, temperature and R_{rs} were collected at stations as well as underway.

e. Tampa Bay:

1) April 17, 1998

2) USGS-funded ship time, NOAA-funded aircraft time

3) Remote sensing reflectance (R_{rs}) and a_g; a_p, a_g, and a_d were measured from the particles captured on filter pads on board R/V Gilbert, on board Twin Oter aircraft AOL, ADAS, and SAS instruments were used.

f. Cobop98:

1) May 15 to June 3, 1998

2) ONR-funded ship time

3) Measurement transects were made offshore from Lee Stocking Island (Bahamas), as well sampling over sandy areas, seagrass areas, coral reef areas, and in the Exuma Sound. Transects from Tampa Bay to and from the Bahamas provided additional, deep water data.

4) Participants aboard the Suncoaster were Ken Carder, David English, Jennifer Patch, James Ivey, Lisa Young, Herschel Hochman, Dennis Nadeau, Larry Langebrake, James Patten, Rob Waterbury, Joe Kuntz, Reed Christenson, and John Kloske. In addition to traditional hydrographic measurements, the Suncoaster collected both apparent optical properties (AOP) and inherent optical properties (IOP) information. AOP's such as upwelling and downwelling radiance and irradiance, and remote-sensing reflectance were

collected at 512 wavelengths. IOP's such as in-water attenuation, absorption, fluorescence, and scattering measurements were obtained from depth profiling packages. Spectral pad absorption was collected due to determine the absorption to phytoplankton and other particles. An autonomous underwater vehicle (AUV) was used to collect upwelling radiance, downwelling irradiance, as well as bottom video imagery at six spectral channels. An instrument that maps bottom microtopography and one that counts different sizes of suspended particles were sucessfully tested aboard AUVs. At Lee Stocking Island, Chris Cattrall collected sky radiance spectral Ed and atmospheric transmission measurements. On the R/V Subchaser, Tom Peacock, David Costello, and Weilin Hou collected water column AOP and IOP profiles and bottom reflectances using the suite of optical instruments on the Rosebud ROV.

g. ECOHAB:

1) June 8 – 12, 1998
2) NOAA-funded ship time
3) Transects over the West Florida shelf
4) Angela Strub participated in the cruise, measuring remote sensing reflectance and a_g; a_p, a_g, and a_d were measured from the particles captured on filter pads.

2. A paper entitled ‘Satellite-Sensor Calibration, Verification Using The Cloud-Shadow Method’ by P. Reinersman, K. Carder, and F.R. Chen, submitted to Applied Optics, is now in press.

An atmospheric-correction and sensor calibration method which uses cloud-shaded pixels together with pixels in a neighboring region of similar optical properties is described for use with high-resolution(e.g. 30m pixels) satellite or aircraft data. This cloud-shadow method uses the difference between the total radiance values observed at the sensor for these two regions, thus removing the nearly identical atmospheric radiance contributions to the two signals(e.g. path radiance and Fresnel-reflected skylight). What remains is largely due to solar photons backscattered from beneath the sea to dominate the residual signal. Normalization by the direct solar irradiance reaching the sea surface and correction for some second-order effects provides the remote-sensing reflectance to the ocean at the location of the neighbor region, providing a known "ground target" reflectance spectrum for use in testing the calibration of the sensor.

A similar approach may be useful for land targets if horizontal homogeneity of scene reflectance exists about the shadow. Monte Carlo calculations have been used to correct for adjacency effects and to estimate the differences in the sky light reaching the shadowed and neighbor pixels.

3. A paper entitled 'Semi-Analytic MODIS Algorithms for Chlorophyll *a* and Absorption with Bio-Optical Domains Based on Nitrogen-Depletion Temperatures' by K. L. Carder, F. R. Chen, Z. P. Lee, S. Hawes , and D. Kamykowski is submitted to JGR has been accepted with revision for publication.

This work describes MODIS algorithms for chlorophyll *a* concentration and phytoplankton and gelbstoff absorption coefficients. The algorithms are based on a semi-analytical, bio-optical model of remote-sensing reflectance, $R_{rs}(\lambda)$, where $R_{rs}(\lambda)$ is defined as the water-leaving radiance, $L_w(\lambda)$, divided by the downwelling irradiance just above the sea surface,

$E_d(\lambda,0^+)$. The $R_{rs}(\lambda)$ model has two free parameters, the absorption coefficient due to phytoplankton at 675 nm, $a_\varphi(675)$, and the absorption coefficient due to gelbstoff at 400 nm, $a_g(400)$. The R_{rs} model has several other parameters which are fixed, or can be specified based on the region and season of the MODIS scene. R_{rs} is modeled using these parameters at each of the visible-range MODIS wavelengths, λ_i. $R_{rs}(\lambda_i)$ is derived at each pixel from the normalized water-leaving radiance, $L_{wn}(\lambda_i)$, measured by MODIS. These $R_{rs}(\lambda_i)$ values are put into the model, the model is inverted, and $a_\varphi(675)$ and $a_g(400)$ are computed. Chlorophyll *a* concentration is then derived simply from the $a_\varphi(675)$ value. For waters with high chlorophyll *a* concentrations where $R_{rs}(412)$ and $R_{rs}(443)$are very low and the algorithm is insensitive, an empirical algorithm with $R_{rs}(488)$ and $R_{rs}(551)$ is used to estimate chlorophyll *a*. The algorithm also outputs both the total absorption coefficients, $a(\lambda_i)$, and the phytoplankton absorption coefficients, $a_\varphi(\lambda_i)$, at the visible MODIS wavelengths. Since absorption per unit chlorophyll varies by a factor of five or more for the global ocean due to accessory pigment-to-chlorophyll variations and pigment packaging or self-shading, to derive accurate chlorophyll *a* concentrations based upon MODIS estimates of absorption, the MODIS algorithms are parameterized for three different bio-optical domains: 1) unpackaged; 2) transitional; and 3) packaged. These provide a variation in domain type from high-light, warm conditions to lower-light, cool conditions and can be identified from space by comparing sea-surface temperature to nitrogen-depletion temperatures(NDTs) for each domain. Algorithm errors of more than 45% for unpartitioned data are reduced to errors of less than 30% for partitoned data with this approach, with the greatest effect occurring at the eastern and polar boundaries of the basins.

To partition data from the NASA SeaWiFS SeaBASS archive into one for regions where little pigment packaging is to be expected but high ratios of photoprotective pigments to

chlorophyll concentrations are found (e.g., high-light, non-upwelling locations in warm, tropical and subtropical waters), versus locations with more packaging and little photoprotective pigments(e.g., eastern boundary upwelling, and non-summer, high latitude sites) two numerical filters were used.

The first numerical filter compares regional field data sets to the CZCS chlorophyll pigment algorithm ($C = 1.14\ [r_{25}]^{-1.71}$, $r_{25} = R_{rs}(443)/R_{rs}(551)$) to check for consistency with this classical algorithm for Case 1 waters, which was developed with largely subtropical and summer temperate data.

The second numerical filter uses the ratios $r_{12}(= R_{rs}(412)/R_{rs}(443))$ and r_{25}. For waters with unpackaged pigments, the line $r_{12} = 0.95\ [r_{25}]^{0.16}$ was used to separate high-gelbstoff data points from the Case 1 data. Based upon the measured a_g data, the gelbstoff-rich Case 2 data had $a_g(400)$ values typically in excess of the relationship $0.12\ [\text{chl } a]^{0.7}$.

Those data sets generally found to be consistent with the CZCS algorithm line as well as occurring above the line $r_{12} = 0.95\ [r_{25}]^{0.16}$ for points where $r_{25} > 3.0$, were classified as "unpackaged", and these consisted of tropical and subtropical data away from eastern-basin boundaries.

There are 287 data points in this ensemble data set: 134 USF data points and 37 EqPac equatorial Pacific points, all measured above-surface and processed using the Lee et al. (1996) protocols; and 126 EqPac points, all measured below-surface using the Mueller and Austin (1995) protocols.

There are 326 points in an ensemble of multi-year, multi-season data sets from the California Current which we label as "packaged." These consist of CalCOFI (n=303) and Cal9704 (n=23) data. The CalCOFI R_{rs} data were subsurface while the Cal9704 data were above-

surface collections. The algorithm yielded RMS1 (log fractional) and RMS2 (linear) errors for chl *a* retrieval of 0.111 and 0.268, respectively when tested with this data set.

To generate an algorithm to transition between regions and periods with packaged and unpackaged pigments, we developed a global data set combining the "packaged", "unpackaged", and other mixed data sets from the SeaBASS archive. This data set has 976 data points, and the algorithm yielded RMS1 and RMS2 errors in algorithm-derived chl *a* of 0.176 and 0.446, respectively.

While algorithms appropriate for regions with packaged or unpackaged pigments can reduce the uncertainty in chlorophyll-a concentration from perhaps 45-50% to less than 30%, methods based upon space-derived data to determine when and where to apply the appropriate parameterization are still under development. A numerical filter has already been discussed, but it is only definitive for waters where $r_{25} > 3.0$ and when no uncertainty in atmospheric correction exists. Also, stations with high gelbstoff concentrations can cause confusion with this method. For offshore oligotrophic to mesotrophic waters, however, it is a very useful diagnostic tool.

A second space-based approach uses the fact that unpackaged pigments are usually found in high-light, nutrient-poor waters where small-diameter phytoplankton cells with high concentrations of photoprotective pigment predominate. Since dissolved nutrients cannot be detected from space, a nutrient surrogate was sought.

Kamykowski (1987) developed a model that explained much of the global covariance observed between upper-layer temperatures and nitrate concentrations. Kamykowski has since developed nitrate-depletion temperatures (NDTs) for the north Atlantic Ocean. These NDTs provide a means to observe from space a variable that indicates when and where nitrate may be limiting phytoplankton growth, and where upper-layer production is dependent upon recycled

nitrogen. Such phytoplankton are typically small with unpackaged pigments and with high photoprotective-chlorophyll pigment ratios.

To delimit regions of the north Atlantic Ocean with unpackaged pigments, we have compared sea-surface temperatures to Kamykowski's NDTs. Fig ure 1 shows annual trends in sea-surface temperature (SST), CZCS pigment, and NDTs for the Gulf of Maine, Bermuda, and Barbados. The temperatures and pigments are four-year (1982-85) monthly averages from the AVHRR and CZCS sensors.

Clearly, the Gulf of Maine is a lower-light, higher-nutrient environment than are Bermuda and Barbados, so the degree of packaging there is likely to be much higher, and the chlorophyll-specific absorption coefficient much smaller. By analyzing bio-optical data in the SeaWiFS SeaBASS archive, some preliminary functional relationships between the NDTs and pigment-packaging classifications for the north Atlantic Ocean were empirically derived using sea-surface temperature (SST) derived from the AVHRR satellite sensor:

<u>DOMAIN</u>:

1. Unpackaged: $SST > NDT + 3.0^{o}$ C

2. Transitional or global: $NDT + 1.8^{o}$ C $< SST < NDT + 3.0^{o}$ C

3. Packaged: $SST < NDT + 1.8^{o}$ C

Using AVHRR SST data from the physical-oceanographic data archive, bio-optical data were sorted into domains using NDTs. Data for the transition period from spring to summer from the NASA SeaBASS archive for the cruises MLML2, AMT4, GOMEX1, GOMEX2, and the North Sea were sorted into the three bio-optical domains, and the appropriate algorithm parameterization was applied to derive chlorophyll *a* values. Atlantic Meridional Transect (AMT

4) data along 20^{o} W longitude collected in May, North Sea data and MLML2 data collected in July, and GOMEX1 and GOMEX2 data collected in April and June provide a diverse set of north Atlantic observations that were sorted by the NDT filter and processed. The results are compared to those obtained by simple use of the global (transitional) algorithm. The RMS1 and RMS2 errors for this diverse data set were 0.153 and 38%, respectively, for domain-sorted data, while the errors grew to 0.186 and 50%, respectively, when processed using global or transitional parameterization for the algorithm without sorting by domain. Some of the error in the domain sorting routine may derive from using monthly composites of AVHRR temperatures rather than weekly values as planned for MODIS.

In summary a semi-analytical algorithm was tested using a total of 976 global data points from regions where the pigments were typically unpackaged, transitional or packaged with appropriate algorithm parameters applied for each data type.

The semi-analytical algorithm performed superbly on each of the data sets after classification, resulting in RMS1 errors of 0.102 and 0.111 (e.g. 0.10 log unit), for the unpackaged and packaged data classes, respectively, with little bias and with slopes near 1.0. RMS2 errors for the algorithms were 24% and 28%, respectively.

For the difficult transition period between spring and summer, a data set was tested that included the eastern-boundary upwelling region of the north Atlantic. The nitrogen-depletion temperature was used with AVHRR-derived sea-surface temperature to sort stations into “packaged”, “unpackaged”, and transitional domains. RMS2 errors dropped from 50% to 38% as a result of this data-sorting exercise. Since large regions of the subtropical Atlantic and Pacific oceans remain in the “unpackaged” bio-optical domain during all seasons and provide rather stable data with accuracies from 24% to 28%, it seems reasonable to expect that use of an NDT-

based sorting algorithm with MODIS sea-surface temperatures to separate data into appropriate bio-optical domains will result in accuracies for the MODIS semi-analytical chlorophyll *a* algorithm that are significantly lower than our target value of 35%.

This study is being expanded to include all oceans and a model parameterization for hyperpackaged pigments found in low-light, high-latitude environments has been developed for addition to the algorithm.

4. A paper entitled 'Empirical Ocean Color Algorithms for Absorption Coefficients of Optically Deep Waters' by Z.P. Lee, K.L. Carder, R.G. Steward, T.G. Peacock, C.O. Davis and J.S. Patch has been revised for publication in JGR.

Since the late 1970's, many empirical algorithms have been developed for chlorophyll-a or pigment concentrations for waters from open ocean to coastal environments, but only a few algorithms have been developed for optical properties of the water. Applying a specific optical property (e.g., specific absorption coefficient), those concentrations can however be converted to absorption and/or attenuation coefficients. As demonstrated, in-water optical properties can be empirically derived from ratios of water-leaving radiance or ratios of remote-sensing reflectance in one step. To extend our early studies, total absorption coefficients at 440 nm ($a_t(440)$, see Notation for symbols used in this text) for the ocean, and those for surface pigment and for gelbstoff are empirically related to the ratios of remote-sensing reflectance at the SeaWiFS bands, which provide alternatives to the pigment-concentration algorithms for deriving in-water optical information.

The total absorption coefficient of surface water, which dominates the variance of both remote-sensing reflectance and the diffuse attenuation coefficients, is important to many aspects of oceanography (e.g., water-type classification, subsurface light intensity, heat flux, etc.).

Empirical algorithms, based on in-water measurements, have been developed for the derivation of the diffuse attenuation coefficient, which closely related to the total absorption coefficient. As the relationship between remote-sensing reflectance and absorption only weakly depends on the solar elevation, the spectral ratios of remote-sensing reflectance data should then be almost independent of solar and/or view angles. This suggests that inherent optical properties such as the total absorption coefficients might be derived from the ratios of remote-sensing reflectance. Based on smaller data sets than the present one, Carder et al. [1992] and Lee [1994] proposed an $a_t(490)$ algorithm using the ratio of remote-sensing reflectance at 520 and 560 nm. Since pigment absorption peaks near 440nm, the values of $a_t(440)$ are instead empirically related to various spectral ratios of remote-sensing reflectance in this study. Actually, field data show that optical properties at 440 and 490nm (e.g., $K_d(440)$ and $K_d(490)$, c(440) and c(490)) are all highly correlated.

The pigment absorption coefficient is important for the calculation of light harvesting by phytoplankton pigments for use in primary production models and for determination of the chlorophyll-a/pigment concentration. Traditional remote sensing methods have estimated pigment absorption using two steps: 1) derive chlorophyll-a or pigment concentration from empirical remote-sensing algorithms; and 2) convert the concentration values to absorption values using known or assumed chlorophyll-specific absorption coefficients. That perhaps accounts for the different empirical and semi-analytical algorithms developed for remote sensing of pigment concentrations. We may, however, get the pigment absorption coefficients directly from the remotely measured data as briefly indicated in Lee et al. [1996a]. This type of algorithm may be applied to a wider range of oceanic environments than the two-step algorithms, since the

chlorophyll specific-absorption coefficient is not involved, which varies widely from place to place.

Gelbstoff absorption coefficients can be used as a tracer of land runoff for coastal environments. No simple remote-sensing algorithm yet exists for the gelbstoff absorption coefficient, but more complex analytical and semi-analytical approaches have been used.

An analytical method has been developed for the derivation of oceanic absorption coefficients from above-surface remote-sensing reflectance. The method uses an optimization approach with hyperspectral data, which would take a rather long calculation time for processing of a satellite image. It is, however, more accurate in decomposing the total absorption coefficients into those of pigment and gelbstoff. For image processing purposes, more rapid algorithms are needed, though they may be less accurate. Recently, Hoge and Lyon [1996] suggested a matrix inversion technique. The technique requires, however, pre-knowledge of the spectral models of the inherent optical properties, and the method has not been tested with field data.

In this study, empirical algorithms are developed for quickly estimating the coefficients at 440nm for total absorption, pigment absorption, and gelbstoff absorption by directly relating them to the ratios of remote-sensing reflectance at two or three of the SeaWiFS wavelength bands. We adopt a formula of cubic polynomials using two spectral ratios. With derived absorption coefficients at 440 nm, the absorption spectrum of the total, the pigment, and the gelbstoff in the visible domain can be constructed using the approaches of Austin and Petzold [1986], Lee [1994], Bricaud et al. [1981], and/or Carder et al. [1991].

5. A paper entitled 'Hyperspectral Remote Sensing for Shallow Waters: 1. A Semi-analytical Model' by Z.P. Lee, K.L. Carder, C. D. Mobley, R.G. Steward, and J.S. Patch has been submitted to Applied Optics for publishing.

Single or quasi-single scattering theory and numerical simulations show that subsurface upwelling signals (SUS) can generally be expressed as a sum of contributions from the water column and from the bottom:

$$SUS_{-} \approx SUS^{dp}\left[1-e^{-2KH}\right]+ SUS^{B}\, e^{-2KH} \qquad (\mathbf{1})$$

Here SUS_{-} can be designated either the subsurface upwelling radiance (L_{u-}), the subsurface irradiance reflectance (R_{-}), or the subsurface remote-sensing reflectance (r_{rs}); we use "subsurface" to mean "just below the air-water surface." SUS^{dp} is for optically deep waters, while SUS^{B} is for the upwelling signals just above the bottom. H is the depth of the water. K is usually described as an "effective attenuation" coefficient.

The first term on the right side of Eq.1 is the water column contribution, though in some studies this term was replaced by a nearby deep-water signal. The second term is the bottom contribution.

Because "effective" attenuation coefficient is ambiguous and hard to determine from remotely measured data, and because the diffuse-attenuation coefficient for downwelling light is not necessarily equal to the diffuse attenuation coefficients for upwelling light, a more general expression for subsurface remote-sensing reflectance, r_{rs}, might be,

$$r_{rs} \approx r_{rs}^{dp}\left[1 - e^{-(K_d + K_u^C)H}\right] + \frac{\rho}{\pi} e^{-(K_d + K_u^B)H}, \quad (2)$$

where K_d is the vertically-averaged-diffuse-attenuation coefficient for downwelling irradiance, K_u^C is the vertically-averaged-diffuse-attenuation coefficient for upwelling radiance from water column scattering, and K_u^B is the vertically-averaged-diffuse-attenuation coefficient for upwelling radiance from bottom reflectance. ρ is the bottom irradiance reflectance, and the bottom is assumed to be a Lambertian reflector.

If we define

$$\kappa \equiv a + b_b, \quad (3)$$

then, to first order, the diffuse attenuation coefficient K is related to κ through a light distribution function (D):

$$K = D\,\kappa. \quad (4)$$

In particular,

$$K_d = D_d\,\kappa, \quad K_u^C = D_u^C\,\kappa, \quad K_u^B = D_u^B\,\kappa, \quad (5)$$

and we can rewrite Eq. 2 as

$$r_{rs} \approx r_{rs}^{dp}\left[1 - e^{-(D_d + D_u^C)\kappa H}\right] + \frac{\rho}{\pi} e^{-(D_d + D_u^B)\kappa H} \quad (\mathbf{6})$$

Note that κ is an inherent optical property. Thus all of the variability in the *K*'s associated with the directional structure of the light field is now transferred to the light distribution functions (*D*).

In many previous remote-sensing applications it was assumed that $D_d = D_u^C = D_u^B$ = a constant, which is equivalent to using a constant "effective" attenuation coefficient (*K*). However, studies of the sub-surface light field suggest that in general $D_d \neq D_u^C \neq D_u^B \neq$ constant, and that the *D*'s vary with the inherent optical properties of the water column. Incorrect assumptions for the values of the *D*'s will cause errors in water-depth derivations. To improve remote sensing of shallow-water bathymetry, for instance, how *D* varies with in-water optical properties needs to be more accurately spelled out.

In this study, the *Hydrolight* numerical model was used to compute above-surface remote-sensing reflectance (R_{rs}) values for a series of water, bottom type, sky, and depth parameters. From these calculated R_{rs} values, parameterizations of *D* were empirically derived, and a semi-analytical model (SA-model) was developed for R_{rs} of deep and shallow waters. This model is invertable for calculation of depths and the optical properties of the water column, where as *Hydrolight* is strictly a numerical forward model and not explicitly invertable.

6. An abstract entitled "Methods for Utilizing Hyperspectral In-situ Light Profiles in the Presence of Wave Focusing and the Absence of above-water Measurements" by D K Costello, K L Carder and J S Patch was presented at the Feb., 98 meeting of the AGU in San Diego meeting.

In simple models (e.g. black sky, smooth surface, homogenous deep water column), underwater light fields decay exponentially with depth. However, the complications which often arise in real measurements are demonstrated using hyperspectral (512 channel) light profiles obtained in the Florida Current. These data show amplitude perturbations in both upwelling radiance (L_u) and downwelling irradiance (E_d) spectra. These perturbations in L_u and E_d are sometimes temporally coherent (e.g. clouds) but are most often incoherent (e.g. wave focusing effects) with the greatest oscillations in E_d. Furthermore, it is particularly apparent in derived E_d data that wave focusing has not only significant amplitude but also significant spectral effects.

2nd-order polynomial fits (P-fits) of $\log(L_u)$ and $\log(E_d)$ as functions of depth were generated to smooth L_u and E_d amplitude fluctuations while allowing for IOP changes and inelastic scattering effects. The zero-order, P-fit coefficient extrapolates the spectra to the water surface, the first-order coefficient is equivalent to the average, spectral diffuse attenuation coefficient, and the second-order coefficient describes the change in attenuation with depth.

The K_u spectra (derived from P-fit-smoothed L_u data) increased with depth at the blue end of the spectrum and decreased at the red end with a distinct “hinge point” at 544 nm. The blue change is attributed to a decreasing particle reflectance (supported by ancillary c-meter data) while the red change is attributed to the increasing importance of water-Raman scattering with depth. The smoothed E_d spectra were significantly improved. Raw curves were evaluated by modelling $E_d(z,\lambda)$ to depth requiring different degrees of focusing on the direct and diffuse irradiance components. Note: K_u and K_d spectra are used to extrapolate underwater measurements of E_d and L_u to the surface for comparison to satellite measurements of normalized water-leaving radiance.

7. An abstract entitled ‘Characterization of Bottom Albedo Using Landsat TM Imagery’ by Renadette, L.A., K.L. Carder, D.K. Costello, W. Hou, D.C. English was presented AGU San Diego meeting.

Using Landsat TM data, we characterized the bottom types along the coast of the Florida Keys. Traditional methods of bottom interpretation, such as spectral unmixing, are not well suited to the limited number of spectral channels provided by Landsat. However, by applying a previously developed histogram-analysis method, we characterized Landsat pixels as sand, seagrass, or fractions thereof. This method was developed using spatial variations in radiance brightness, collected over regions of variable bottom composition. In situ measurements of water optical properties and bottom reflectance end members (pure bright sand, thick dark grass) allow us to verify our results. Our results suggest that histogram analysis of satellite data can be a simple and effective means of estimating and removing path radiance from a scene, and characterizing bottom albedos if the bottom depth is known.

8. An abstract entitled ‘Characterizations and Techniques needed for the use of Spectral Radiometers to Collect Plane Irradiance Measurements’ by D. C. English, R. G. Steward, D. K. Costello, K. L. Carder is presented at AGU San Diego meeting.

Spectral plane irradiance measurements, especially downwelling plane irradiance measurements, are important to understanding the distribution of light in water and interpreting reflectance measurements both above and below the water surface. While attempting to characterize radiant and irradiant spectrometers developed at the University of South Florida (USF) we have confronted several problems in collecting accurate spectral irradiance measurements, including a commercial spectral radiometer with previously understated angular

response errors. We compare the results of several different techniques for obtaining downward irradiance values and present the directional response of the cosine collectors used with the USF spectrometers. We offer recommendations for sensor characterization and the collection of spectral irradiance measurements.

9. An abstract entitled 'Effects of Colored Dissolved Organic Matter (CDOM) and Pigment Packaging on Remote Sensing Reflectance Algorithms in the Southeastern Bering Sea' by Patch, J.S., Carder, K.L., Lee, Z.P., Steward, R.G was presented at the AGU, San Diego meeting.

Current remote sensing algorithms for obtaining pigment concentrations from SeaWiFS and other ocean-viewing sensors have been developed primarily for Case I waters. In such waters, the absorption due to colored dissolved organic matter (CDOM) covaries with pigment concentration. The southeastern Bering Sea is a region where this covariation no longer holds true. Regional algorithms that recognize this lack of covariance and that also take into account pigment packaging are required in low-light, high latitude areas such as the Bering Sea in order to more accurately estimate pigment concentration compared to high-light, subtropical algorithms. In this study, remote-sensing reflectance ratios for SeaWiFS wavelength bands are related to each other and to inherent optical properties (aph, ag, and fluorometrically measured chlorophyll a concentration) of surface waters. Shipboard data were collected during April 1996 in the southeastern Bering Sea and the Alaskan Current as part of a NOAA sponsored Fisheries Oceanography Coordinated Investigations (FOCI) program. A numerical filter approach for identifying high CDOM and highly packaged stations based solely on Rrs ratios is examined. An empirical model relating ag(440) and reflectance ratios involving wavelength bands centered at 412, 443, 490, and 555nm is developed.

10. An abstract entitled “The Modulation of Optical Properties of Sombrero Key, Florida” by J. E. Ivey, K. L. Carder, H. Hochman, J. Patch, and R. G. Steward was submitted for presentation at the SPIE “Ocean Optics” conference in Hawaii, Oct 14-17, 1998.

A study of the optical properties of Sombrero Key reef was made from 28 June to 1 July 1997. The attenuation coefficient at 440 nm of the color constituents of water near Sombrero Key was dominated by scattering (b =0.19 m^{-1}) while constituent absorption at 440 nm was only 0.07 m^{-1}. The high b:a ratio is possibly the result of re-suspension of sediment by wave action. The constituent absorption value (a(412) = 0.25 m^{-1}) in Hawk Channel, between Sombrero Key reef and Florida Bay, was much greater than on the adjacent reef (a(412) = 0.07 m^{-1}). This warm, saline, particle-rich water appeared to be trapped at depth in the channel as a result of higher density (1022.6 kg m^{-3} vs. 1022.4 kg m^{-3}), ultimately flowing out through cuts in the reef rather than over the reef top. The ag(412) values were 85% of the constituent absorption coefficients over Sombrero Key Reef while it contributed only 65% to constituent absorption for Hawk Channel. The relatively high ag(412) values (e.g. 0.06 m^{-3}) found over the reef may aid in limiting UV penetration to the coral at depth (> 8m) and may limit possible UV effects on coral bleaching.

11. An abstract entitled “Variability in the Inherent Optical Properties for the Northeastern Gulf of Mexico: Application to a Semi-Analytical Ocean Color Algorithm” by Patch, Jennifer S., Carder, Kendall L; Steward, Robert G, Kirkpatrick, Gary J. was submitted for presentation at the SPIE “Ocean Optics” conference in Hawaii, Oct 14-17, 1998

Chlorophyll *a* concentrations in the Northeastern Gulf of Mexico during an August 1997 cruise spanned nearly two orders of magnitude ranging from 0.13 mg m^{-3} to 4.3 mg m^{-3}. The relative contributions of a_{ph}, a_d, and a_g to the total non-water absorption coefficient at 443nm remained relatively constant over this entire range at 40%, 10%, and 50%, respectively. HPLC data, however, indicates a taxonomic shift from blue-green algae and prymnesiophytes dominating the offshore stations to diatoms dominating the riverine stations. This shift is accompanied by changes in pigment packaging due to variations in size and internal pigment concentrations along with differences in accessory pigment types and concentrations as observed in the $a_{ph}(443)/a_{ph}(675)$ ratio. Understanding these changes is crucial for increasing the accuracy of remote-sensing algorithms that derive ocean color constituents. The slope and magnitude of the gelbstoff absorption curves also differed between these two regions with lower slopes and values occurring offshore compared to higher slopes and values occurring near the riverine outflow. The goal here is to discuss how regional variations in inherent optical properties necessitate the implementation of regional parameters in the Carder semi-analytical algorithm for optimal ocean color constituent retrievals. A modification in the algorithm is made in order to obtain optical closure with regard to the gelbstoff slope variable. Stations with increased pheopigments relative to chlorophyll *a* require increased gelbstoff slopes as this slope parameter includes effects due to the sum of the absorption contributions of gelbstoff, detritus, and pheopigments. How these parameters vary with hydrological properties will be discussed along with how they may be possibly implemented.

12. An abstract entitled " An Evaluation Of Bottom Interpretation From Space Using Underwater Imagery" by Renadette, Lisa A. ; Carder, Kendall L.; Costello, David K.; Hou, Weilin and Zhang,

Mingrui, was submitted for presentation at the SPIE “Ocean Optics” conference in Hawaii, Oct 14-17, 1998

We use bottom imagery from a remotely-operated vehicle (ROV) and an autonomous underwater vehicle (AUV) to develop algorithms for interpretation of bottom characteristics from space. Imagery from spaceborne sensors are simulated by combining AUV images for areas equivalent to Landsat or Coastal Ocean Imaging Spectrometer (COIS) pixels (30m). Pixels with variable mixtures of sand and seagrass are simulated. Near-surface imagery is analyzed to estimate pixel-area fractions of sand and seagrass for spectral channels of atmospherically-corrected, high-resolution satellite data. Albedo end members for sand and seagrass are established with near-bottom ROV imagery; path radiance and path attenuation coefficients are determined using vertical ROV profiles. Using this approach, we evaluate the viability of bottom interpretation from space and its potential applications in assessment and management of coastal flora and fauna.

13. An abstract entitled “A Neural Network Approach to Deriving Optical Properties and Depths of Shallow Waters “ by Z. P. Lee, M. R. Zhang, K. L. Carder, and L. O. Hall was submitted for presentation at the SPIE “Ocean Optics” conference in Hawaii, Oct 14-17, 1998

A Neural Network (NN) approach is studied in deriving information on the bathymetry and water column properties for optically shallow waters. In this study, more than 2000 remote-sensing reflectance (ratio of water-leaving radiance to downwelling irradiance above the surface) spectra for shallow waters were created with a semi-analytical model. This synthetic database covered chlorophyll-a concentrations from 0.2 to 5 mg/m^3, water depths from 0.5 to 20 meters, and dark to bright-sand bottom albedos. The multi-layer NN is trained with the synthetic data

base using a back-propagation algorithm, and tested with field measurements. One advantage of using a NN approach is that it reduces the calculation time greatly compared to an early optimization method.

14. An paper entitled “Optical Model of Long-Range aharan Dust For Use in Ocean Color Imagery As Determined By In-Situ Radiometric Measurements” by Christopher Catrall, K. Crader was submitted for presentation at the SPIE “Ocean Optics” conference in Hawaii, Oct 14-17, 1998

Sky radiance and aerosol optical depth measurements have been taken in the Dry Tortugas, Florida, during two summer dust episodes where Saharan dust dominates the aerosol optical properties. The data are inverted using the Wang and Gordon algorithm to determine the single-scattering albedo and phase function of Saharan dust that has undergone such long range transportation. Aerosol vertical distributions from previous lidar measurements of Saharan dust over the Atlantic are used in the retrieval.

Preliminary results suggest distinct spectral absorption at wavelengths less than 620 nm, with the albedo decreasing sharply in the blue (380 - 490 nm) wavelengths, and a phase function possessing flattened side-scattering behaviour. The robustness of the optical model is investigated using identical measurements performed at the Bahamas and the Dry Tortugas when a mix of marine and Saharan dust aerosols was present.

The presence of mineral dust possessing an albedo much less
than unity and strong spectral dependence severely degrades atmospheric correction of ocean colour imagery and derived chlorophyll pigment concentration. In-situ determination of the optical properties of absorbing aerosols is a key issue in improving

the quality of atmospheric correction. We suggest the optical model may be added to the candidate aerosol models used to generate atmospheric correction algorithms.

15. An Abstract entitled “Detecting Desert Dust Storms Using SeaWiFS Images” by Kendall L. Carder , F. Robert Chen, Christopher Catrall, and Angela Straub was submitted for presentation at the SPIE “Ocean Optics” conference in Hawaii, Oct 14-17, 1998

SeaWiFS images can be used to map major desert dust events as they spread over the ocean. During these events, CZCS images of Saharan Dust have shown that the aerosol reflectance is lower in the blue than the green or red end of the spectrum. In particular, $\varepsilon(550,670)$, the ratio of the 550 and 670 nm aerosol reflectances, was less than 0.94 for large, iron-rich desert dust particles. The aerosol reflectance is defined as aerosol scattered radiance divided by the cosine of the solar zenith angle and the extraterrestrial solar irradiance. Determination of $\varepsilon(550,670)$ is based on the fact that the total radiance measured at the sensor is the sum of the aerosol, Rayleigh, and water-leaving radiance. Rayleigh radiance is predictable. For optically-deep, clear water regions (chlorophyll a concentrations less than 0.25 mg/m^3), the normalized water-leaving radiances at 550 and 670 nm can be designated *a priori* to be 0.28 and less than 0.015 $mw/cm^2/sr/um$, respectively. Removal of these two components allows the aerosol radiance to be derived from the SeaWiFS measurements.

Accurate maps of desert dust dispersal are important to the atmospheric correction for ocean color sensor such as SeaWiFS. Since it signals blue-absorbing aerosols in the atmosphere. Accurate estimation of the water-leaving radiance in the blue end of the spectrum is crucial to determination of the chlorophyll a concentration and primary production.

References:

Biggar, S.F., and K.J. Thome, 'Solar-radiation-based Absolute Calibration of Optical Sensors: SeaWiFS and a Daedalus 1268, IGARSS-94, Pasadena, California.

Publications:

P. Reinersman, P., K. Carder, and F.R. Chen, 'Satellite-Sensor Calibration, Verification Using The Cloud-Shadow Method', Vol. 37, No.24, Applied Optics, 20 Aug. 1998.

Anticipated Activities:

1. The relationships between temperature anomalies and nutrients in regard to the packaging effect will be explored in order to reduce uncertainty in the chlorophyll algorithm using Bering Sea data and upwelling data from the Arabian Sea , Monterey Bay, Southern California Bight, and the East China Sea.

2. Research expeditions to be completed:

a) Yellow Sea cruise

   1) June 20-July 15, 1998

   2) Chinese Science Bureau funded ship time

   3) Turbid water optics.

a. South China Sea cruise

   1) October 2-October 22, 1998

   2) Taiwanese Science Counsel funded ship time

   3) MODIS cal/val.

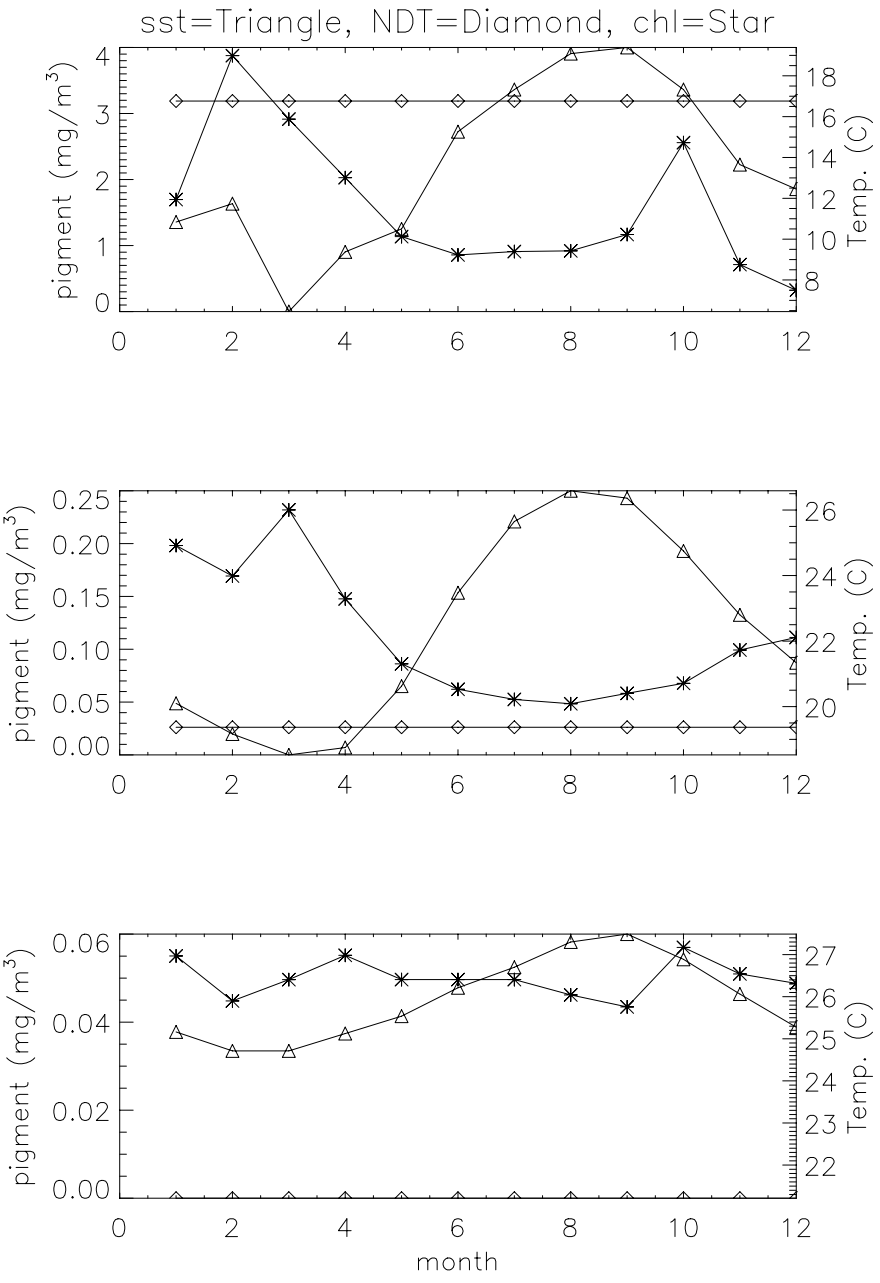

Figure 1: Four-year (1982-1985), monthly-mean values of Sea-surface temperature (triangles), CZCS pigment (asterisks), and nitrate-depletion temperature (diamonds) for locations near a) the Gulf of Maine, b) Bermuda, and c) Barbados.